Jour. Comp. & App. Res. in Mech. Eng. Vol. 10. No. 2, pp. 1-10, 2021 *DOI: 10.22061/jcarme.2019.4665.1564*

SRTTU

Journal of Computational and Applied Research in Mechanical Engineering

jcarme.sru.ac.ir

JCARME

ISSN: 2228-7922

Efficient approaches to reduce cavitation damage risk in the bottom outlet: Case study of Seymareh dam

Tohid Jamali Rovesht[a] and Mohammad Manafpour[b, *]

[a]*Department of ArGEnCo, Research Group Hydraulics in Environmental and Civil Engineering (HECE), Liège University, Liège, Belgium.*
[b]*Department of Civil Engineering, Faculty of Engineering, Urmia University, Urmia, Iran.*

Article info:

Article history:

Received: 00/00/0000
Accepted: 00/00/0018
Revised: 00/00/0000
Online: 00/00/0000

Keywords:
Cavitation mitigation
Dam safety
Geometrical optimization
Numerical investigation
Flow3D

[*]Corresponding author:
m.manafpour@urmia.ac.ir

Abstract

The occurrence of the cavitation phenomenon in hydraulic structures operating under high flow velocities remains a critical challenge. Efficient mitigation strategies may include increasing air concentration and optimizing the geometric design, such as minimizing sharp changes in flow direction and reducing local vortices. The Seymareh dam bottom outlet, operating under high water heads, is prone to cavitation due to its velocity and pressure fields. This study numerically investigates the effects of geometric modifications on cavitation risk reduction. Results showed that removing lateral expansion increases cavitation indices on outlet walls, while designing a concave curved bed elevates pressure and cavitation indices on the bed surface. Nonetheless, implementing both modifications together completely suppresses cavitation risk. The numerical analysis was conducted under single-phase flow conditions, without considering air entrainment, which, in practice, could further improve outlet safety. These findings could provide useful insights for geometric design approaches to control cavitation in high-velocity hydraulic structures.

1. Introduction

Bottom outlets in dams can experience substantial operational issues such as cavitation, vibrations in the control gates, and obstructions caused by blockages [1-3]. These challenges can affect hydraulic performance and the structural integrity of the outlet system. Cavitation arises due to negative pressures and elevated flow velocities along the outlet surfaces [4-6]. Increasing flow velocity hinders the flow's adaptation to the lateral wall expansion, which strengthens local vortices, reduces the pressure, and ultimately increases the risk of cavitation. Li *et al.* [7] observed cavitation occurrence at a lateral expansion angle of 2.23° under partial gate openings. Some studies have reported cavitation occurrence at specific lateral expansion angles under various gate openings [8-10] and have proposed criteria ($\tan\alpha \leq (3Fr)^{-1}$, α = maximum expansion angle and Fr = Fr number) combining maximum wall

expansion angle and Froude number to prevent flow separation [11].

Previous research has identified flow aeration and geometric modifications as effective strategies for reducing cavitation damage [12, 13]. Dong *et al.* [14] reported that negative pressure values in the cavitation zone of the bottom outlet were recovered remarkably by increasing the airflow concentration. The numerical study conducted by Salazar *et al.* [15] demonstrated that the maximum airflow rate passing through the aerator duct into the bottom outlet flow scales proportionally with approximately 80% of the opening of the service gate. Experimental findings by Abdolahpour and Roshan [16] revealed cavitation indices increased in bottom outlet beds where the slope transitioned from horizontal to an adverse inclination of 7.7°.

In another experimental investigation, Roun Shi *et al.* [17]. demonstrated that decreasing the bed slope downstream of the aerator enhanced air entrainment into the flow, effectively safeguarding the bottom outlet surfaces from cavitation damage. Furthermore, Li *et al.* [18] showed the cavitation index on outlet sidewalls remained below 0.2 for all lateral expansion angles, even at zero expansion, with partial gate openings and a Froude number of 2.92, with similar findings across various gate openings and a Froude number of 4.29.

Additionally, advanced numerical approaches have been widely employed to analyze high-speed flows and cavitation phenomena in hydraulic structures. In particular, the K-ε (RNG) turbulence model coupled with the Volume of Fluid (VOF) method has proven effective in simulating complex two-phase flows. Jamali *et al.* [19] evaluated cavitation indices along the sidewalls under varying flow conditions and different lateral wall expansions. Li *et al.* [20] simulated aerated flow in a curved connecting tunnel, while Dargahi [21] analyzed the flow behavior in bottom outlets equipped with moving gates. Li *et al.* [22] further examined the downstream hydraulics of a radial gate incorporating a sudden lateral expansion and a vertical bottom drop. Sha *et al.* [23] also investigated high-velocity flow in a spillway tunnel. Jamali *et al.* [24] examined how flow conditions and chute geometry influence shockwave formation on chute spillways.

A prior study on the Seymareh dam bottom outlet highlighted significant cavitation risks along the bed and sidewalls downstream of the service gate across different gate openings [25]. High flow velocity (Fr = 20.05), a 12° wall expansion, and insufficient aeration were identified as the primary factors driving this phenomenon.

This study numerically evaluated the impact of geometric modifications on cavitation risk in a high-velocity dam bottom outlet, using the Seymareh dam as a prototype. Three scenarios were analyzed to assess their effects on cavitation indices along the bed and sidewalls: removal of wall expansion to reduce local pressure drops, implementation of a concave bed to increase pressure, and a combination of both strategies. A conservative single-phase CFD approach was employed to isolate the influence of geometry on cavitation inception (Fig. 1).

The results are benchmark redesign options for high-velocity dam bottom outlets with cavitation damage risk and provide practical guidelines for geometric optimization, enhancing hydraulic efficiency, and informing future CFD and experimental investigations of cavitation-prone structures.

2. Fundamental equations of fluid flow

The incompressible turbulent flow with uniform properties is governed by the conservation equations for mass and momentum, given in Eqs. (1 and 2) [26]:

$$\frac{\partial U_i}{\partial x_i}=0 \tag{1}$$

$$\frac{\partial U_i}{\partial t}+U_j\frac{\partial U_i}{\partial x_j}=-\frac{1}{\rho}\frac{\partial \overline{P}}{\partial x_i}+\frac{\partial}{\partial x_j}\left(\nu\frac{\partial U_i}{\partial x_j}-\overline{u_i'u_j'}\right) \tag{2}$$

Here, x_i defines the spatial position, t represents the temporal evolution, and ρ indicates the material density. Variables $\bar{P}$, $\bar{U}_i$, u_i', and u_j' quantify time-averaged pressure, velocity field, and turbulent stress contributions, respectively.

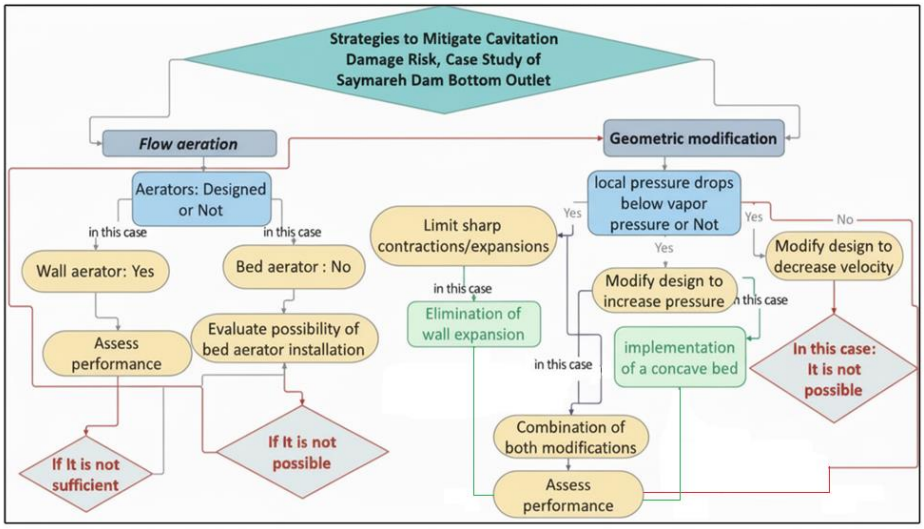

Fig. 1. Flowchart of approaches to reduce cavitation damage risk in Seymareh dam bottom outlet.

To capture the water surface, a volume-fraction approach via the VOF technique is utilized, employing indicator F to represent liquid filling within computational cells. The evolution of F obeys the transport equations in Eqs. (3 and 4).

$$\frac{\partial F}{\partial t}+\frac{1}{V_F}\left[\frac{\partial}{\partial x}(FA_x u)+R\frac{\partial}{\partial y}(FA_y v)\right]+\frac{1}{V_F}\left[\frac{\partial}{\partial z}(FA_z w)+\xi\frac{FA_x u}{x}\right]=F_{DIF}+F_{SOR} \quad (3)$$

$$F_{DIF}=\frac{1}{V_F}\left[\frac{\partial}{\partial x}\left(\upsilon_F A_X\frac{\partial F}{\partial x}+R\frac{\partial}{\partial x}\left(\upsilon_F A_y R\frac{\partial F}{\partial y}\right)\right)\right]+\frac{1}{V_F}\left[\frac{\partial}{\partial z}\left(\upsilon_F A_z\frac{\partial F}{\partial z}\right)+\xi\left(\frac{\upsilon_F A_X F}{X}\right)\right] \quad (4)$$

In these equations, V_F quantifies the partial cell filling, (u, v, w) specify the convective transport, and A_x A_y A_z provide the geometric weighting. Cartesian grids simplify relations $(R = 1, \xi = 0)$, while F_{SOR} accommodates the phase change. Liquid fills cells where $F = 1$; $F = 0$ identifies gas/vapor pockets of negligible mass [27, 28].

3. Prototype configuration and laboratory setup

Seymareh arch dam incorporates dual bottom outlets, Fig. 2(a-b), positioned at 620 m and 640 m elevation above sea level (20 m, 40 m above tailwater).

This study focuses on bottom outlet No. 1 (total length 45.4 m), transitioning from a pressurized section (36.5 m) to a free-surface flow section (8.9 m) (Fig. 3(a-b)). The outlet is designed to deliver a maximum discharge of 654 m³/s under an upstream head of 111.5 m.

Laboratory testing utilized a 1:15 Froude-scaled model at Iran Water Resources Management Co. (Tehran) (Fig. 4). Wall pressures were measured via Seventy-four piezometers, discharges quantified by a calibrated sharp-crested weir, and the upstream waterhead was monitored using a vertical manometer. Experiments were conducted for multiple gate openings and two different upstream heads.

a)

b)

Fig. 2. (a) Seymareh dam and (b) related hydraulic structures [29].

a)

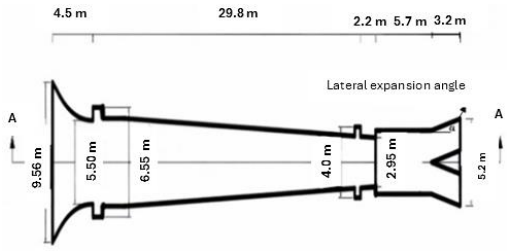

b)

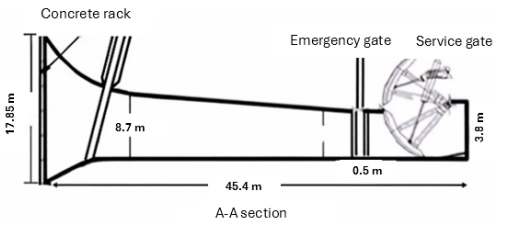

Fig. 3. (a) Top view and (b) cross-sectional view of bottom outlet No. 1 at Seymareh dam.

a)

b)

c)

d)

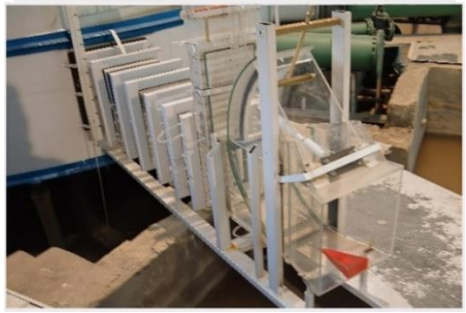

Fig. 4. Physical model of the Seymareh dam bottom outlet: (a) bottom outlet entrance, (b) emergency and service gates, (c) bottom outlet configuration and geometry, (d) downstream region of the service gate.

4. Computational setup and verification

A three-dimensional numerical model of the bottom outlet was developed using FLOW-3D software. The full-scale geometry was generated in AutoCAD 3D and exported in STL format. The fluid was assumed to be incompressible. Inlet boundary conditions corresponded to the reservoir head, while outflow and wall boundary conditions were applied at the outlet and walls, respectively. Turbulence was modeled using the RNG (k-ε) approach, and the VOF method was employed to capture the free-surface profile. The computational domain consisted of 1,506,019 mesh cells, and simulations were run for 30 s.

To determine suitable upstream conditions, the model was tested using different reservoir dimensions (Table 1).

Table 1. Reservoir sensitivity cases.

Reservoir no.	Reservoir dimensions (width×length m^2)	Number of computational mesh
1	10× 9.53	50,592
2	20× 19.53	219,443
3	30× 29.53	507,500
4	40× 39.53	884,268
5	45× 44.53	1,126,650

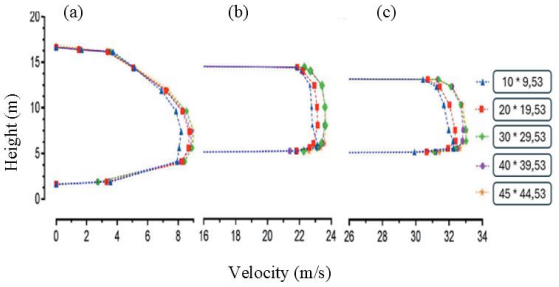

Fig. 5. Flow velocity distributions at sections located (a) 2 m, (b) 20 m, and (c) 30 m downstream of the outlet entrance for various reservoir dimensions.

The flow velocity fields at three sections of the outlet revealed negligible differences for the largest three reservoir sizes, selecting the 30 × 29.53 m² reservoir as optimal (Fig. 5). Validation of the numerical model was performed by comparing mean bed pressures with experimental measurements for upstream heads of 100 m and gate openings of 30%, 70%, and 100% (Fig. 6(a-c)). High correlation coefficients confirmed that the numerical model reliably reproduces the observed physical flow behavior.

5. Results and discussion

5.1. Existing hydraulic conditions of the bottom outlet

Analysis of the existing hydraulic conditions of the bottom outlet indicates that cavitation along the bed and sidewalls poses a significant damage risk [19]. For gate openings of 10%, 20%, 30%, 40%, and 80%, the cavitation index (σ) drops below the critical threshold of 0.2 between X = 41 m and the downstream end (Fig. 7 (a, b)), and from X = 41 m to X = 43 m for 50% and 70% openings.

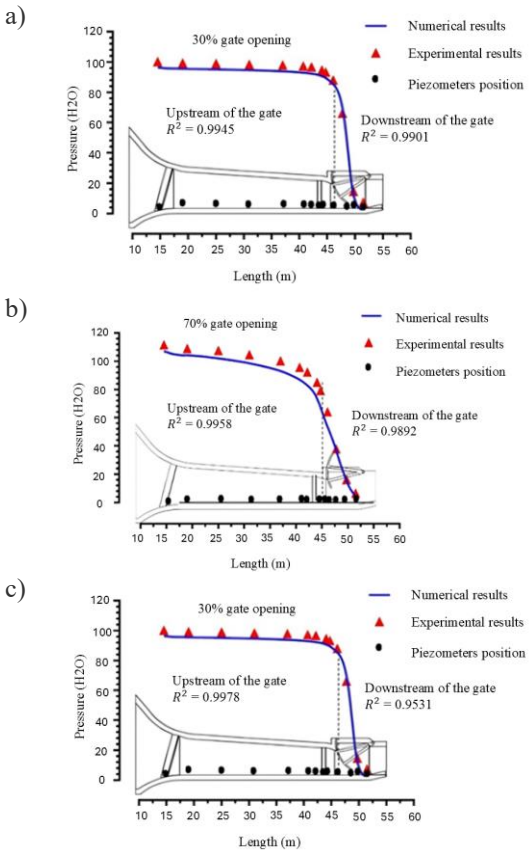

Fig. 6. Comparison of mean bed pressure for gate openings of (a) 30%, (b) 70%, and (c) 100% between numerical simulations and experimental measurements.

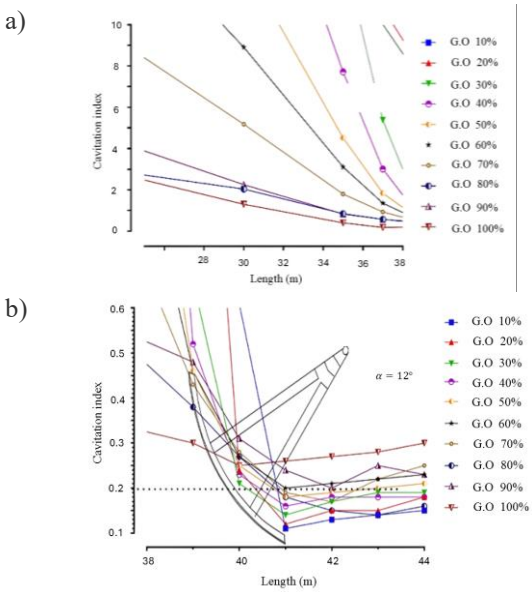

Fig. 7. Distribution of the cavitation index (σ) along the outlet bed for various service gate openings: (a) upstream of the gate and (b) downstream of the gate.

This behaviour occurs due to the rapid acceleration of flow and the resulting pressure drop near the service gate, which is caused by the contraction of the outlet section. In the free-surface region, the flow struggles to adapt to the lateral expansion of the sidewalls, further worsened by inadequate sidewall aeration.

The outlet sidewalls are also susceptible to cavitation. Fig. 8(a, b) illustrates that at X = 41 m, the cavitation index (σ) drops below the critical threshold of 0.2 for all gate openings except when the gate is fully open (100%). Furthermore, at X = 42 m, the cavitation index (σ) along the sidewalls stays below 0.2 across all service gate openings.

The maximum Froude number (Fr = 20.05) is observed at the initial phase of lateral expansion of the sidewalls for the critical 10% service gate opening (Fig. 9).

According to the formulas proposed in the literature ($\tan\alpha \leq (3Fr)^{-1}$), the recommended maximum expansion angle for the outlet walls should be zero under these hydraulic conditions. However, an actual wall angle of 12° was implemented in the design, which prevented the flow from properly adjusting to the sudden lateral expansion. This geometric discrepancy resulted in flow separation, the development of local vortices, and ultimately the onset of cavitation in the region downstream of the gate.

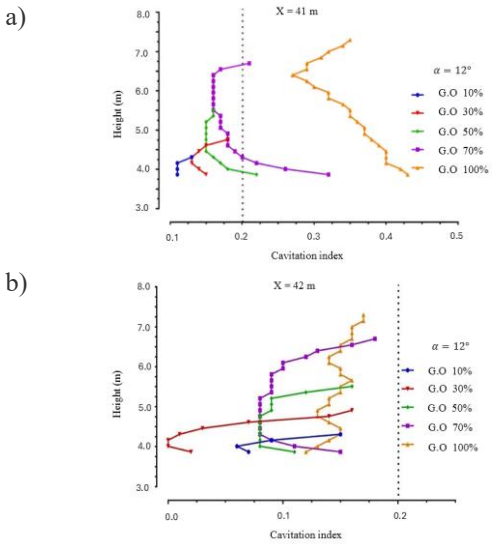

Fig. 8. Cavitation index (σ) distribution along the outlet sidewalls for different gate openings at sections (a) X = 41 m and (b) X = 42 m.

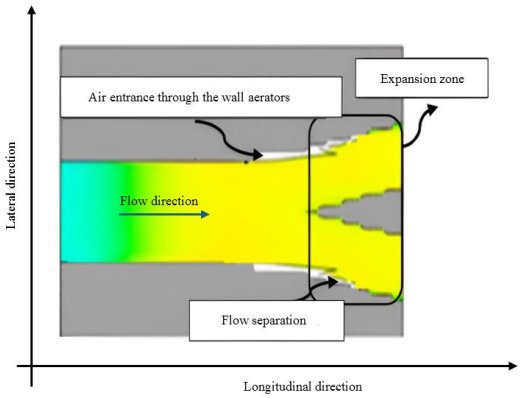

Fig. 9. Flow pattern in the free-surface region.

5.2. Effective approaches for reducing cavitation damage

5.2.1. Aeration

5.2.1.1. Aeration by a wall aerator

In the Seymareh bottom outlet, the radial service gate is installed on side supports where air cavities develop, effectively acting as outlet wall aerators. Fig. 10 illustrates that increasing the gate lift enlarges the cavities, thereby enhancing air entrainment in the free-surface flow.

Field observations indicate that the wall aerators are insufficient in mitigating cavitation damage, with some deterioration already present at the downstream end of the outlet. This highlights the need to reduce the lateral expansion angle of the outlet sidewalls, which currently exceeds the permissible limit.

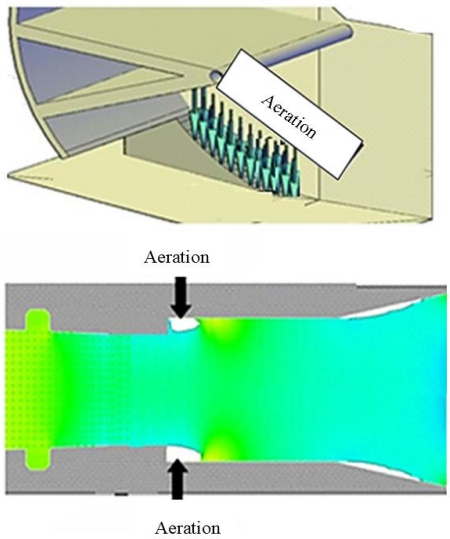

Fig. 10. Schematic of the wall aerator downstream of the gate.

5.2.1.2. Aeration using a bed aerator

In this case, no bed aerator is employed to avoid potential damage to the outlet bed. The outlet relies solely on wall aerators, whose performance is inadequate. These wall aerators cannot fully aerate the flow across the outlet width near the bed, as the aerated zone develops gradually from the sidewalls toward the centerline, requiring a considerable distance to cover the full width. Meanwhile, cavitation occurs immediately downstream of the service gate along the outlet bed (Fig. 7), indicating the necessity of a bottom aerator.

The bed aerator should be installed immediately downstream of the service gate lip, with its position varying according to the gate opening (within a range of 4.6 m in the flow direction). Installing the aerator downstream of the service gate (when the gate is fully closed) exposes the upstream side of the gate to cavitation. As the gate lifts, its tip moves upstream, and a high-velocity flow develops before reaching the bed aerator. Conversely, placing the aerator upstream of the gate leads to undesirable gate vibrations and surface oscillations at the terminal structure. Therefore, the installation of a bed aerator in this configuration is not feasible (Table 2).

Table 2. Aeration approach to reduce cavitation damage risk.

Approach	Type	In this case	Results
Aeration	Wall aerator	Designed	Not sufficient
	Bed aerator	Not designed	Not feasible

5.2.2. Geometric modifications

Mitigating cavitation damage risk requires increasing the local pressure or reducing the flow velocity while suppressing vortex formation. However, reducing the flow velocity is generally impractical in this context, as it is controlled by the upstream reservoir head. To mitigate vortex-induced pressure depressions, abrupt planform or cross-sectional changes that encourage flow separation should be avoided. In practice, decreasing the free-surface expansion angle reduces side-wall detachment. Additionally, adopting a concave outlet-bed profile (like a flip bucket) can introduce centrifugal effects along the curvature, thereby elevating the mean bed pressure and increasing the cavitation index (Table 3) [30, 31]. In this bottom outlet, a concave bed profile 9.4 m in length has been proposed, starting at the service gate lip (100% gate opening) and extending to the outlet end (Fig. 11). The radius of curvature (R) has been set to 18 m, calculated for the fully open gate condition using the criterion $4D \leq R$ (D = hydraulic depth).

Table 3. Geometric modifications to reduce cavitation damage risk.

Approach	Type	In this case	Results
Geometric modifications	Decrease flow velocity	Controlled by upstream reservoir head	Not feasible
	Restrict sharp contractions/ expansions	Wall expansion elimination	……..
	Enhance flow pressure	Implementation of a concave bed	……..
	Restrict sharp contractions/ expansions + enhance flow pressure	Integrated modifications	……..

The critical cavitation zone beneath the service gate ($L_1 = 4.6$ m, covering the range of gate lip positions) has been replaced with a 6° ramp instead of the proposed concave bed (Fig. 11), resulting in higher mean pressures than the curved profile. The ramp angle was selected based on conventional spillway aerator ramps, which are typically less than 10° [32].

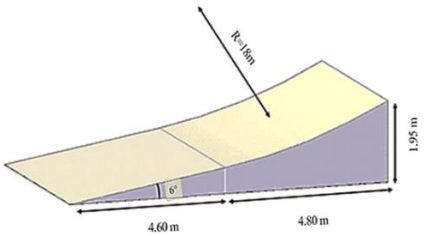

Fig. 11. Sketch of the geometric modifications.

5.2.2.1. Wall Expansion Elimination

Based on the criterion proposed in the literature ($\tan \alpha \leq (3\,\mathrm{Fr})^{-1}$), the outlet sidewall expansion was set to 0°, and the cavitation index (σ) was numerically evaluated for the most critical condition, corresponding to a 10% service gate opening, according to the physical

model results. The results show that the cavitation indices remain below the critical range, varying between 0.12 and 0.22 (Fig. 12). However, σ values have increased significantly compared to the existing outlet condition (Fig. 8), rising from nearly zero to values above 0.13.

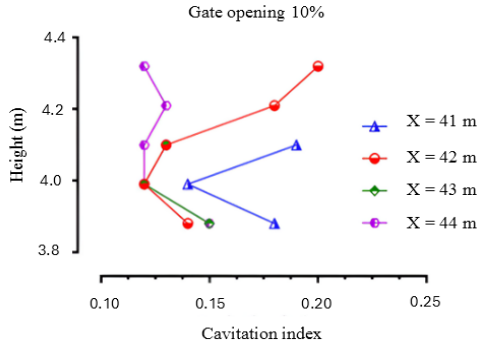

Fig. 12. Variation of σ along the outlet sidewall at 10% service gate opening following the removal of wall expansion.

Furthermore, this geometric modification of the sidewalls slightly reduced the cavitation index (σ) along the outlet bed across different gate openings. As illustrated in Fig. 13, compared with the existing condition shown in Fig. 7, σ decreased from 0.3 to 0.22 at full gate opening and from 0.15 to 0.12 at 10% gate opening. This can be explained by comparing the flow fields in both scenarios, which show that mean pressures remain largely steady downstream of the gate, while flow velocities increase slightly due to the elimination of wall expansion (Table 4).

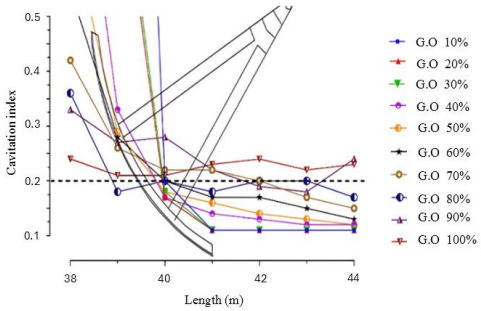

Fig. 13. σ variation on outlet bed for different service gate openings after eliminating wall expansion.

5.2.2.2. Implementation of a concave bed

The concave bed was applied in the free-surface section. Evaluation of σ across different gate openings shows that all values exceed the critical limit of 0.2, increasing by approximately 20% compared to the initial outlet (Fig. 14 vs Fig. 7). To assess the effect of bed modification on sidewall cavitation, σ was evaluated along the sidewalls. The results (Fig. 15) indicate an increase in σ (Table 4), with the largest differences occurring near the outlet bed compared to the initial design (Fig. 8). For instance, at a section 42 m from the outlet entrance, the minimum cavitation indices for gate openings of 10%, 30%, 50%, and 70% increased from 0.05, 0.10, 0.08, and 0.09 to 0.12, 0.14, 0.13, and 0.15, respectively.

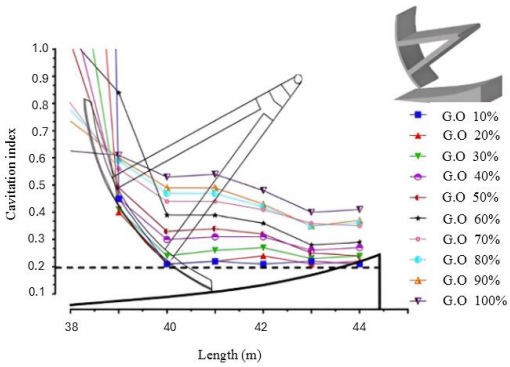

Fig. 14. σ variation on the outlet bed for various gate openings after bed geometry modification.

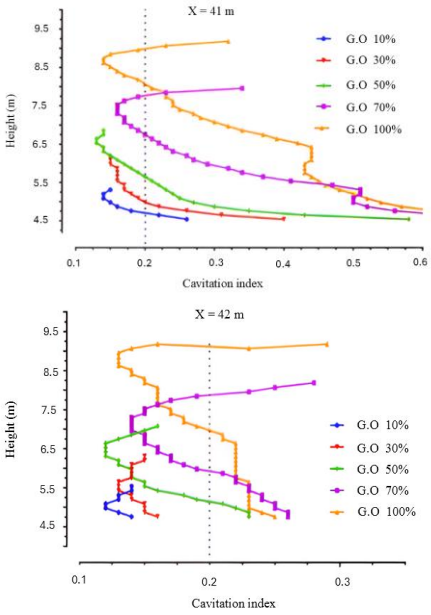

Fig. 15. σ variation along outlet sidewall at (a) X = 41 m, and (b) X = 42 m for various gate openings after bed geometry modification.

Applying the proposed geometric modifications increases σ along the outlet bed and sidewalls, and their combined application enhances flow conditions, effectively reducing the risk of cavitation.

5.2.2.3. Integrated modifications

Figs. 16 and 17 show the variation of σ on the outlet sidewalls and bed after simultaneous modifications on the bed and sidewalls. The results indicate that σ values generally exceed the critical threshold of 0.2 (Table 4), approximately doubling relative to the initial outlet (Fig. 8). However, some indices decrease to 0.19, particularly at the upper levels of the side walls. It should be noted that the numerical simulation assumes single-phase flow. In practice, the flow transitions to a free surface immediately downstream of the service gate and is significantly aerated by the sidewall aerators, reducing the risk of cavitation damage.
Compared with the initial outlet results (Fig. 7), σ on the outlet bed has approximately doubled for partial gate openings and tripled for large gate openings, as shown in Fig. 16. The minimum cavitation index occurred at 10% gate opening with a value of 0.2, which is acceptable in terms of cavitation damage risk and could be further mitigated in practice through aeration via the sidewall aerators.

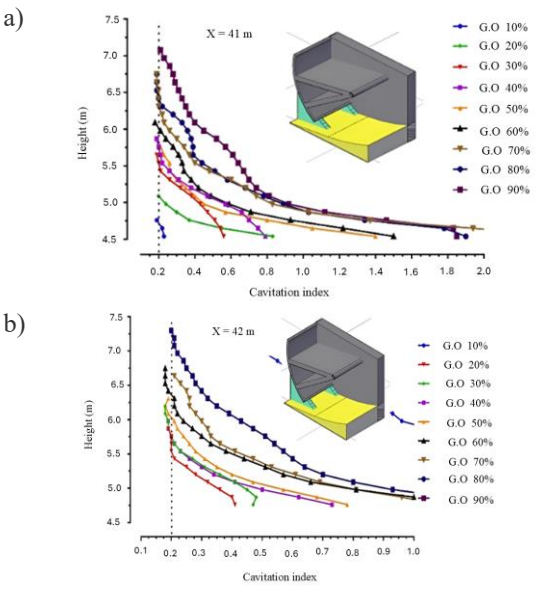

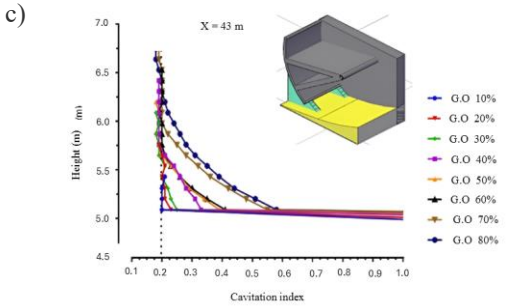

Fig. 16. σ variation on outlet sidewalls at (a) X = 41 m, (b) X = 42 m, and (c) X = 43 m for different gate openings following bed and side wall geometry modifications.

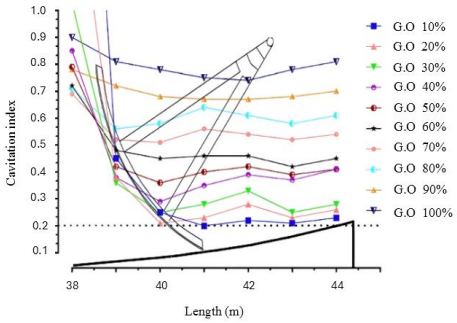

Fig. 17. σ variation on the outlet bed for various gate openings following bed and side wall geometry modifications.

Table 4. Summary of geometric modifications to reduce cavitation damage.

Approach	Type	In this case	Results
Geometric modifications	Decrease flow velocity	Controlled by upstream reservoir head	Not feasible
	Restrict sharp contractions/ expansions	Wall expansion elimination	Side wall σ ↑ but insufficient; bed σ ↓
	Enhance flow pressure	Implementation of a concave bed	Side wall σ ↑ but insufficient; bed σ ↑ but insufficient
	Restrict sharp contractions/ expansions + enhance flow pressure	Integrated modifications	Side wall σ ↑; bed σ ↑, both were sufficient

6. Conclusions

This study examined geometric modifications to mitigate cavitation risk in high-velocity dam bottom outlets, using the Seymareh dam as a case study. Results indicate that cavitation susceptibility in these flows arises from the

interplay of hydraulic conditions, aeration performance, and structural geometry.

The effectiveness of traditional sidewall aeration is compromised when the entrained air–water mixture does not achieve full cross-sectional coverage, creating zones susceptible to cavitation and erosion. Targeted geometric adjustments—such as minimizing wall expansion angles and adopting a concave bed profile—markedly elevate local cavitation indices and eliminate low-pressure regions prone to damage. Although adjustments to the bed or sidewalls alone yield only marginal gains, optimal mitigation is achieved through integrated optimization of both boundaries.

In summary, effective cavitation control in high-velocity dam outlets demands a dual strategy: (i) geometric optimization to suppress local vortices, elevate pressures, and minimize velocity (where feasible), and (ii) targeted aeration in vulnerable zones. This integrated design paradigm unifies aeration and outlet geometry, boosting hydraulic efficiency, prolonging service life, and guiding CFD/experimental studies on cavitation-prone structures.

7. Acknowledgments

This paper is derived from the first author's M.Sc. thesis, entitled “Numerical Investigation of Flow Patterns at the Bottom Outlet (Case Study: Seymareh dam),” carried out at Urmia University, Iran. The authors gratefully acknowledge Urmia University for providing the resources and facilities necessary to conduct this research. Appreciation is also extended to the Water Resources Management Company, the Ministry of Energy of Iran for providing the physical model report of the Seymareh dam's bottom outlet.

8. References

[1] M. Zounemat-Kermani, T. Rajaee, A. Ramezani-Charmahineh, and J. F. Adamowski, “Estimating the aeration coefficient and air demand in bottom outlet outlets of dams using GEP and decision tree methods,” *Flow Meas. Instrum.*, Vol. 54, pp. 9–19, (2016).

[2] W. Wei and J. Deng, “Wedge aerator at the bottom outlet in flat tunnels,” *J. Hydraul. Eng.*, Vol. 149, No. 1, Art. no. 04022037, (2022).

[3] G. H. Chen, G. Y. Wang, C. L. Hu, B. Huang, and M. D. Zhang, “Observations and measurements on unsteady cavitating flows using a simultaneous sampling approach,” *Exp. Fluids*, Vol. 56, No. 2, Art. 32, (2015).

[4] G. Wang, Q. Wu, and B. Huang, “Dynamics of cavitation–structure interaction,” *Acta Mech. Sin.*, Vol. 33, No. 4, pp. 685–708, (2017).

[5] V. V. Bhosekar, V. Jothiprakash, and P. B. Deolalikar, “Orifice spillway aerator: hydraulic design,” *J. Hydraul. Eng.*, Vol. 138, No. 6, pp. 563–572, (2012).

[6] A. Mohagheg and J. H. Wu, “Effects of hydraulic and geometric parameters on downstream cavity length of discharge tunnel service gate,” *J. Hydrodyn.*, Vol. 21, No. 6, pp. 774–778, (2009).

[7] Sh. Li, J. Zhang, X. Chen, G. Zhou, and J. Chen, “Characteristics of aeration of flow downstream of the radial gate with sudden fall-divergence aerator in discharge tunnel,” *Water Supply*, Vol. 1, No. 3, pp. 790–798, (2017).

[8] G. Lei, H. Huang, X. Fan, J. Su, Q. Wang, X. Wang, and J. Zhang, “Influence of the transition section shape on the cavitation characteristics at the bottom outlet,” *Water Supply*, Vol. 23, No. 8, pp. 3061–3077, (2023).

[9] A. H. Nikseresht, N. Talebbeydokhti, and H. Khorshidi, “Three-dimensional numerical modeling of cavitation and aeration system in dam outlets,” *J. Fluids Eng.*, Vol. 134, No. 9, p. 091302, (2012).

[10] S. Li, J. Zhang, X. Chen, J. Chen, and G. G. D. Zhou, “Cavity length downstream of a sudden fall-expansion aerator in chute,” *Water Supply*, Vol. 18, No. 6, pp. 2053–2062, (2018).

[11] Ph. L. Thompson and R. T. Kilgore, Hydraulic design of energy dissipaters for culverts and channels, 3rd Edition, U.S.

Department of Transportation, pp. 4–4, (2006).
[12] W. H. Hager and R. M. Boes, "Hydraulic structures: a positive outlook into the future," *J. Hydraul. Res.*, Vol. 52, No. 4, pp. 299–310, (2014).
[13] N. Wright and B. Tullis, "Prototype and laboratory low-level outlet air demand comparison for small-to-medium-sized embankment dams," *J. Irrig. Drain. Eng*., Vol. 140, No. 6, pp. 0401–4013, (2014).
[14] Z. Dong, L. Chen, and W. Ju, "Cavitation characteristics of high-velocity flow with and without aeration on the order of 50 m/s," *J. Hydrodyn*., Vol. 19, No. 4, pp. 429–433, (2007).
[15] F. Salazar, J. San-Mauro, M. Celigueta, and E. Onate, "Air demand estimation in bottom outlets with the particle finite element method," *Comput. Part*. Mech., Vol. 4, No. 3, pp. 345–356, (2016).
[16] M. Abdolahpour and R. Roshan, "Flow aeration after gate in bottom outlet tunnels," Arabian *J. Sci. Eng*., Vol. 39, No. 5, pp. 3441–3448, (2014).
[17] P. Ruan Shi, J. Wu, and W. Wu, "Hydraulic research of aerators on tunnel spillways," *J. Hydrodyn*., Vol. 19, No. 3, pp. 330–334, (2005).
[18] S. Li, J. Zhang, W. Xu, J. Chen, and Y. Peng, "Evolution of pressure and cavitation on side walls affected by lateral divergence angle and opening of radial gate," *J. Hydraul. Eng*., Vol. 142, No. 7, p. 05016003, (2016).
[19] T. Jamali, M. Manafpour, and H. Ebrahimnezhadian, "Evolution of pressure and cavitation in transition region walls for supercritical flow," *J. Water Supply Res*. Technol., Vol. 72, No. 1, pp. 62–82, (2023).
[20] Sh. Li, J. Zhang, W. L. Xu, J. Chen, Y. Peng, J. Li, and X. He, "Simulation and experiments of aerated flow in curve connective tunnel with high head and large discharge," *Int. J. Civ. Eng*., Vol. 14, No. 1, pp. 23–33, (2016).
[21] B. Dargahi, "Flow characteristics of bottom outlets with moving gates," *J. Hydraul*. Res., Vol. 48, No. 4, pp. 476–482, (2010).
[22] G. J. Li, G. Q. Dai, Y. Qing, and X. D. Ma, "Detached eddy simulation of hydraulic characteristics along the sidewall after a new arrangement scheme of the sudden lateral enlargement and the vertical drop," *J. Hydrodyn*., Vol. 23, No. 5, pp. 669–675, (2011).
[23] H. Sha, S. Wu, and Z. Chen, "3D numerical simulation for spillway tunnel," *Adv. Water Sci*., Vol. 17, No. 4, pp. 507–511, (2006).
[24] T. Jamali and M. Manafpour, "Investigation on cavitation occurrence potential in Seymareh Dam's bottom outlet," *ISH J. Hydraul. Eng*., Vol. 27, Suppl. 1, pp. 530–541, (2021).
[25] T. J. Rovesht, M. Manafpour, and M. Lotfi, "Effects of flow condition and chute geometry on the shockwaves formed on chute spillway," *Water Supply Res. Technol*., Vol. 71, No. 2, pp. 312–329, (2022).
[26] J. H. Ferziger and M. Peric, Computational Methods for Fluid Dynamics, Springer, Berlin, Heidelberg, (2012).
[27] J. M. Zhang, J. G. Chen, W. L. Xu, Y. R. Wang, and G. J. Li, "Three-dimensional numerical simulation of aerated flows downstream sudden fall aerator expansion in a tunnel," *J. Hydrodyn*., Vol. 23, No. 1, pp. 71–80, (2011).
[28] C. Hirt and B. Nichols, "Volume of fluid (VOF) method for the dynamics of free boundaries," *J. Comput. Phys*., Vol. 39, pp. 201–225, (1981).
[29] Mahab Ghodss Consulting Engineers, Seymareh Dam Project, available at: http://mahabghodss.net/ExternalSites/new/proj_seymareh.aspx.
[30] SA. Tavakkol, A. R. Zarrati, and M. Khanpour, "Curvilinear smoothed particle hydrodynamics," *Int. J. Numer. Methods Fluids*, Vol. 83, No. 2, pp. 115–131, (2016).
[31] M. Pfister, W. H. Hager, and R. M. Boes, "Trajectories and air flow features of ski jump-generated jets," *J. Hydraul. Res*., Vol. 52, No. 3, pp. 336–346, (2014).
[32] H. Fuhrhop, H. E. Schulzh, and H. Wittenberg, "Solution for spillway chute

aeration through bottom aerators," *Int. J. Comput. Methods Exp. Meas*., Vol. 2, No. 3, pp. 298–312, (2014).